Fire resistance of high strength concrete filled steel tubular columns under combined temperature and loading

Chao-Wei Tang [*]

Department of Civil Engineering & Geomatics, Cheng Shiu University,
No. 840, Chengcing Rd.,Niaosong District, Kaohsiung City, Taiwan R.O.C.

Abstract. In recent years, concrete-filled box or tubular columns have been commonly used in high-rise buildings. However, a number of fire test results show that there are significant differences between high strength concrete (HSC) and normal strength concrete (NSC) after being subjected to high temperatures. Therefore, this paper presents an investigation on the fire resistance of HSC filled steel tubular columns (CFTCs) under combined temperature and loading. Two groups of full-size specimens were fabricated to consider the effect of type of concrete infilling (plain and reinforced) and the load level on the fire resistance of CFTCs. Prior to fire test, a constant compressive load (i.e., load level for fire design) was applied to the column specimens. Thermal load was then applied on the column specimens in form of ISO 834 standard fire curve in a large-scale laboratory furnace until the set experiment termination condition was reached. The results demonstrate that the higher the axial load level, the worse the fire resistance. Moreover, in the bar-reinforced concrete-filled steel tubular columns, the presence of rebars not only decreased the spread of cracks and the sudden loss of strength, but also contributed to the load-carrying capacity of the concrete core.

Keywords: fire resistance; high strength concrete; concrete filled steel tubular columns
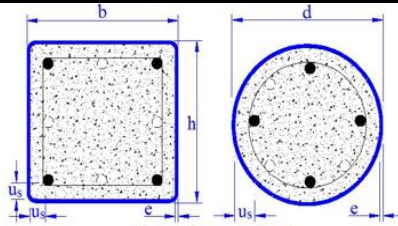
1. Introduction

The definition of high-strength concrete (HSC) varies on a geographical basis. According to the American Concrete Institute, HSCs are those that attain cylinder compressive strength of at least 41 MPa at 28 days (ACI 363R-92 1992). In general, HSC has increased modulus of elasticity, which increases stability and reduces deflection (Jagannath *et al.* 2016). Therefore, HSC has been recently becoming an increasingly popular building material for various applications. Especially, composite columns made of HSC filled steel hollow sections have the advantages of high bearing capacity, large stiffness, good seismic performance, and convenient installation (Liew and Xiong 2015). Moreover, steel reinforced concrete structures have several practical benefits. For instance, compared with bare steel or reinforced concrete columns, the use of concrete-filled box or tubular columns (CFBCs or CFTCs) may have as a relatively small sectional dimension and omission of formwork, which decreases labor and material costs (Han *et al.* 2005, Lavanya and Elangovan 2017, Zhou *et al.* 2017). In addition, the use of composite steel-concrete building elements also results in a high level of fire resistance without the need for fire protection (EN 1994-1-2 2005). Consequently, CFBCs or CFTCs have been applied more extensively in the construction of modern high-rise buildings, bridges, and plants throughout the world over the past few decades (Lie and Kodur 1996, Kodur 1999, Uy 2001, Kodur *et al.* 2004, EN 1994-1-2 2005, Kim *et al.* 2005, Kodur 2007, Ding and Wang 2008, Espinos *et al.* 2009, Hong and Varma 2009, Song *et al.* 2010, Aslani *et al.* 2015, Qu *et al.* 2015, Khan *et al.* 2016, Ekmekyapar 2016, Mago and Hicks 2016, Tao *et al.* 2016, Wan and Zha 2016, Chen *et al.* 2017, Tan and Nichols 2017, Tang and Chen 2017, Tang 2017).

Building fires typically reach temperatures of around 1000°C, which can reduce the loadbearing capacity of structural elements and cause damage or collapse of the structure. Therefore, most building codes stipulate that the structural elements of a building have to satisfy appropriate fire safety requirements (ACI-318 2014, EN 1992-1-2 2004, Kodur 2014). Fire protection features on structural elements are usually measured in terms of fire resistance, which is the ability of a given structural element to perform its design function for a period of time in the event of a fire (Purkiss 2007). Overall, the design rules for the fire resistance of existing structural elements such as steel, concrete, masonry and wood are based entirely on the results and observations of standard fire tests. Traditionally, fire resistance has been evaluated by subjecting a structural element in a furnace for a specified duration (ASTM E119 2008). The resulting fire rating is expressed in time, usually in minutes. In other words, fire rating is used to indicate the time that a structural element can withstand the effects of a standard fire test before reaching the specified destruction criteria. According to the standard fire test results, the fire rating of structural elements is divided into: R30, R60, R90, R120, R180 and other categories.

---

[*]Corresponding author, Ph.D., Professor,
  E-mail: tangcw@gcloud.csu.edu.tw

Table 1 Tabular data for fire design of concrete filled steel tubular columns (EN 1994-1-2 2005)

Typical Concrete Filled
SHS & CHS Cross-Section

	Steel section: $(b/e) \geq 25$ or $(d/e) \geq 25$	R30	R60	R90	R120	R180
1	Minimum cross-sectional dimensions for load level $\eta_{fi,t} \leq 0.28$					
1.1	Minimum dimensions h and b or minimum diameter d [mm]	160	200	220	260	400
1.2	Minimum ratio of reinforcement $A_S/(A_S+A_C)$ in (%)	0	1.5	3.0	6.0	6.0
1.3	Minimum axis distance of reinforcing bars u_s [mm]	-	30	40	50	60
2	Minimum cross-sectional dimensions for load level $\eta_{fi,t} \leq 0.47$					
2.1	Minimum dimensions h and b or minimum diameter d [mm]	260	260	400	450	500
2.2	Minimum ratio of reinforcement $A_S/(A_S+A_C)$ in (%)	0	3.0	6.0	6.0	6.0
2.3	Minimum axis distance of reinforcing bars u_s [mm]	-	30	40	50	60
3	Minimum cross-sectional dimensions for load level $\eta_{fi,t} \leq 0.66$					
3.1	Minimum dimensions h and b or minimum diameter d [mm]	260	450	550	-	-
3.2	Minimum ratio of reinforcement $A_S/(A_S+A_C)$ in (%)	3.0	6.0	6.0	-	-
3.3	Minimum axis distance of reinforcing bars u_s [mm]	25	30	40	-	-

*Notes: $\eta_{fi,t}$ = load level for fire design; F = fiber content (Volume %); R = reinforcement ratio = $A_s/(A_s+A_c)$, A_c = cross-sectional area of the concrete, A_s = cross-sectional area of the reinforcing bars; u_s = minimum axial distance of reinforcing bars

According to Eurocode 4 (EN 1994-1-2 2005), the structural fire design of composite steel and concrete columns consist in three different levels of assessment, namely tabular data, simple calculation models, and general calculation models. The tabulated data method was based on observations resulted from experimental study and was easy to apply. But application of tabulated data is confined to individual structural members, considered as directly to fire over their full length. In addition, thermal action is taken in accordance with standard fire exposure. Moreover, the tabulated data method is valid for columns with a maximum length of 30 times the minimum external dimension of the cross-section chosen. On the other hand, it was for specific types of structural members. In other words, it was limited by the geometrical conditions imposed to the composite cross-section. For example, the tabular data for the fire design of composite columns made of concrete filled steel hollow sections subjected to axial compressive loading are given in Table 1 (EN 1994-1-2 2005). As can be seen in Table 1, the standard fire resistance is found as a function of the load level, $\eta_{fi,t}$, the cross-section size b, h or d, the reinforcement rate, i.e., the ratio between the cross-sectional area of reinforcement and the total area, $A_s/(A_c+A_s)$, and the distance between the reinforcements and internal surface of the steel tube, u_s. The load level for fire design at time t, $\eta_{fi,t}$, is given by

$$\eta_{fi,t} = \frac{E_{fi,d,t}}{R_d} \qquad (1)$$

where $E_{fi,d,t}$ is the design effect of action in the fire situation at time t and R_d is the design resistance for normal temperature design.

Due to its superior and dense microstructure, HSC possesses different mechanical properties compared to normal strength concrete (NSC). However, a great number of fire test results show that there is a significant difference between HSC and NSC at high temperatures. At 20-800℃, HSC has a slightly lower specific heat than NSC (Kodur and Sultan 2003). In particular, HSC elements tend to explosive spalling due to the build-up of pore pressure in dense microstructured HSCs upon exposure to rapidly increasing temperatures (Castillo and Durrani 1990, Sanjayan and Stocks 1993, Phan and Carino 1998, 2002, Hertz 2003, Krzemień and Hagera 2009, Siddique and Kaur 2012, Kodur 2014, Mundhada and Pofale 2015). As a result, the integrity and loadbearing capacity of HSC elements may be reduced. However, as reported by different authors, the reduction in HSC strength at high temperatures is inconsistent and there are significant variations in strength loss (Kodur 2014, Liu *et al.* 2015, Xiong and Liew 2016, Schaumann and Kleibömer 2017).

In view of the above considerations, the present study aimed at conducting an investigation on the fire resistance of high strength concrete filled steel tubular columns under combined temperature and loading. Two groups of full-size specimens were fabricated to consider the effect of type of concrete infilling (plain and reinforced) and the load level on the fire resistance of CFTCs.

Table 2 Design of CFTC specimens and summary of test information

Group type	Specimen No.	$\eta_{fi,t}$	R	u_s (mm)	S (mm)	F_{ys} (MPa)	E_s (GPa)	F_{yr} (MPa)	f_c' (MPa)	Slump (mm)	Slump flow (mm)
Control group	A1	0.28	0	-	-	245.2	205.9		51	235	550
	A2	0.47	0	-	-	245.2	205.9		51	235	550
Experimental group	B1	0.47	6%	40	200	245.2	205.9	525.8	51	235	550
	B2	0.66	6%	40	200	245.2	205.9	525.8	51	235	550

*Notes: $\eta_{fi,t}$ = load level for fire design; R = reinforcement ratio = $A_s/(A_s+A_c)$, A_c = cross-sectional area of the concrete, A_s = cross-sectional area of the reinforcing bars; u_s = minimum axial distance of reinforcing bars; S = stirrup spacing; F_{ys} = yield strength of the steel tube; E_s = steel modulus of elasticity; F_{yr} = yield strength of the reinforcing bars; f_c' = compressive strength of concrete

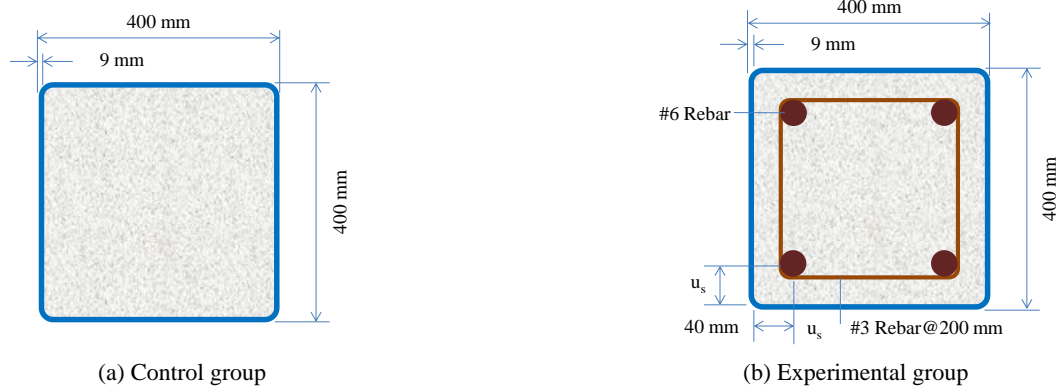
(a) Control group   (b) Experimental group

Fig. 1 Cross section of CFTC specimens

2. Experimental procedure

2.1 Experimental program

In this study, four CFTC specimens consisting of square hollow structural sections filled with HSC were used. The design and planning of the CFTC specimens are given in Table 2. As can be seen from Table 2, two groups of full-size specimens were cast. Each group had two specimens. The control group was filled with plain HSC, while the experimental group was filled with high strength reinforced concrete. The column specimens were made of steel tube and had square cross sections, as shown in Fig. 1. All the columns were 3000 mm long. Moreover, 30-mm-thick end plates were welded to the top and bottom of the columns. In addition, no external fire-proofing was provided for the steel.

2.2 Casting of specimens

Materials used for the core concrete included cement, slag, fly ash, fine aggregates, coarse aggregates, and superplasticizer. The cement used here was Type I Portland cement with a specific gravity of 3.15 and a fineness of 3400 cm²/g. The fine aggregate was natural river sand. The coarse aggregate was siliceous crushed stone with a maximum particle size of 19 mm. The mix proportions for the HSC are shown in Table 3. The slump flow test was adopted to assess the workability of the concrete.

Table 3 Mix proportions of concrete

W/B	Cement (kg/m³)	Slag (kg/m³)	Fly ash (kg/m³)	Water (kg/m³)	FA (kg/m³)	CA (kg/m³)	SP (kg/m³)
0.32	250	140	110	160	836	842	5

*Notes: W/B = water-binder ratio, FA = fine aggregate, CA = coarse aggregate, SP = superplasticizer (HICON MTP A40)

Concrete test specimens were made according to the ASTM C192 specification (ASTM C192/C192M-16a 2016). Freshly mixed concrete was slowly poured in the column specimens by use of a concrete placement bucket and a funnel, followed by controlled vibrations. In addition, twenty-one cylindrical specimens were cast for compressive strength test. All the column specimens and cylinders were covered with a wet hessian and plastic sheets overnight. Then, the cylinders were removed from the molds. Following demolding, the cylinders were immediately submerged in a water curing tank in the laboratory until the time of testing. All the column specimens were placed indoors for 72 days under indoor curing conditions. On the other hands, the compressive strength of three concrete cylinders was tested at ages of 1, 3, 7, 14, 21, 28, and 72 days, respectively.

2.3 Test set up and procedure

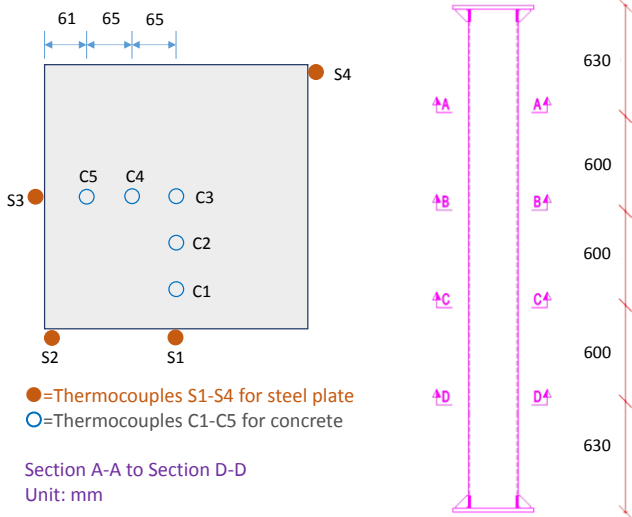To monitor and measure the temperature of the CFTC

Fig. 2 Scheme and thermocouples layout of CFTC

Fig. 3 Installation of the C1-C5 thermocouples for the
control group

Fig. 4 Installation of the C1-C5 thermocouples for the
experimental group

specimens during the fire test, an appropriate number of thermocouples were buried inside and outside the column. The temperature from the CFTC's surface to the inner central core was measured with type K thermocouples. Fig. 2 shows that the thermocouples were placed at different depths in four sections of the column. As can be seen from Fig. 2, nine thermocouples were placed in each section: four (i.e., S1-S4) were welded to the steel tube surface and the five others (i.e., C1-C5) were embedded in the inner concrete at various depths. For the control group, configured the C1-C5 thermocouples in a wire cage, then placed the wire cage in the steel tube (Fig. 3). For the experimental group, the C1-C5 thermocouples were placed in a reinforcement cage, then the reinforcement cage was placed in the steel tube (Fig. 4). A sufficient number of linear variable displacement transducers (LVDTs) were used to measure the axial displacements of the CFTC specimens. They were placed on the top and bottom of the test columns.

Prior to the fire test, the column specimen was installed in the furnace as shown in Fig. 5; and then a constant compressive load (i.e., load level for fire design) was applied to the column specimen. This load was controlled by a load cell of 19.6 MN, located on the head of the piston

of a jack. The applied load corresponded to 28%, 47%, and 0.66% of the nominal compressive strength of the specimen, respectively, which is the design value of the buckling resistance of the column at room temperature. The nominal compressive strength P_n is defined in the Taiwan Design Code for Steel Reinforced Concrete (SRC) Structures (Taiwan Construction and Planning Agency 2004) as

$$P_n = \phi_{cs} P_{ns} + \phi_{crc} P_{nrc} \tag{2}$$

$$P_{ns} = \left(0.211\lambda_c^3 - 0.57\lambda_c^2 - 0.06\lambda_c + 1 \right) F_{ys} A_s \tag{3}$$

$$P_{nrc} = \phi_e \left(0.85 f_c' A_c + A_r F_{yr} \right) \tag{4}$$

$$\lambda_c = \frac{KL}{\pi r_{eff}} \sqrt{\frac{F_{ys}}{E_s}} \tag{5}$$

$$r_{eff} = r_s + \alpha \times \sqrt{\frac{I_g}{A_g}} \tag{6}$$

$$r_s = \sqrt{\frac{I_s}{A_s}} \tag{7}$$

where P_{ns} = nominal steel compressive strength; P_{nrc} = nominal compressive strength of the reinforced concrete of
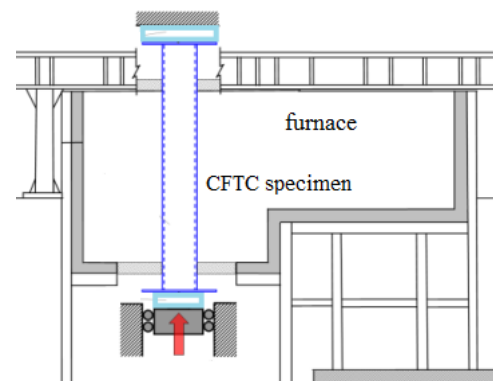

Fig. 5 Test setups for CFTC specimens

the SRC column; ϕ_e, ϕ_{cs}, and ϕ_{crc} = resistance factors: for compression; A_s = area of steel cross section; A_c = area of concrete; A_r = area of longitudinal mild reinforcement; A_g = gross area of the member; F_{ys} = yield strength of steel; F_{yr} = yield strength of longitudinal mild reinforcement; E_s = steel modulus of elasticity; f_c' = concrete strength; λ_c = slenderness parameter; K = effective length factor; L = lateral unbraced length of the member; r_s = governing radius of gyration; α = correction factor for effective radius of gyration; I_s = moment of inertia of steel; I_g = moment of inertia of gross member section.

The ISO 834 standard fire curve was used for the testing of the column specimens in a natural gas-fired large-scale laboratory furnace until the set experiment termination condition was reached. The temperature inside the furnace was controlled by 18 gas burners, and 14 thermocouples were used to monitor the furnace temperature at different locations. The current failure criterion specified in ISO 834 is adopted in this study, which is based on the amount of contraction and the rate of contraction. For the columns under consideration, the strength failure criteria correspond to a maximum contraction of 30.6 mm and a rate of contraction of 9.18 mm/min.

3. Experimental results and discussion

3.1 Compressive strength of cylindrical HSC specimens

Compression testing was performed using a servo-hydraulic material testing system. Mean compressive strength was calculated by taking average of three specimens. The average compressive strength versus curing age for the cylindrical HSC specimens is shown in Fig. 6. It can be seen in Fig. 6 that the compressive strength increased with increasing ages of curing. In addition, the average measured cylinder compressive strength (f_c') on the testing day for the CFTC specimens was 51 MPa. Therefore, the compressive strength of concrete in the CFTC specimens can be regarded as 51 MPa.

3.2 Furnace temperature versus time

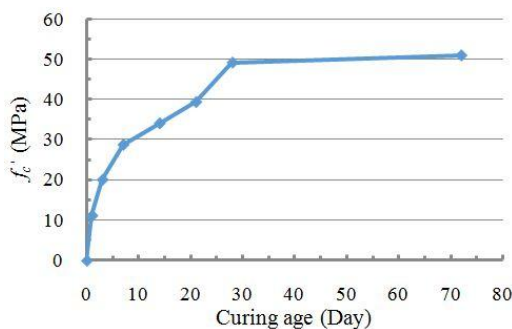Prior to the fire test, the predetermined axial compression load was applied to the column specimens. The load

Fig. 6 Compressive strength of cylindrical HSC specimens versus curing age

Table 4 Test conditions

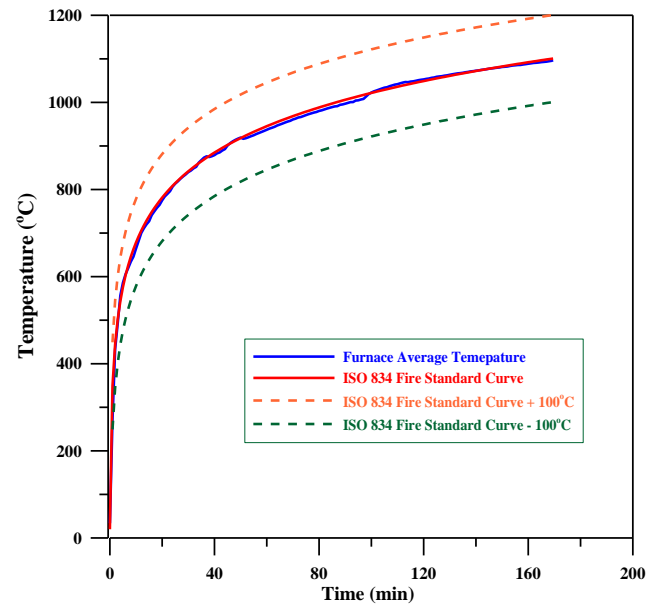| Item	Specimen No.			
	A1	A2	B1	B2
Yield strength of the steel tube (MPa)	245.2	245.2	245.2	245.2
Compressive strength of concrete (MPa)	51	51	51	51
Yield strength of the reinforcing bars (MPa)	-	-	525.8	525.8
Load level for fire design	0.28	0.47	0.47	0.66
Applied axial compressive load (KN)	1752.6	2935.8	2971.4	4119.1

Fig. 7 Temperature versus time curves in the furnace for the A1 specimen

levels for fire design of the A1, A2, B1 and B2 specimens were 0.28, 0.47, 0.47, and 0.66 respectively. According to Eqs. (2)-(7), the applied axial compressive loads were calculated for the control group and the experimental group respectively, as show in Table 4. Then four CFTCs were tested to failure by exposing the loaded columns to fire. During the test, the column was exposed to heating controlled in such a way that the average temperature inside the furnace was as close as possible to the standard time-temperature curve of ISO 834. For example, Fig. 7 shows the furnace temperature in the fire resistance test for the A1 specimen, indicating a precise control of furnace temperature.

3.3 Fire test results

Fire tests were carried out on the CFTC specimens. When the column specimens reached the aforementioned failure criterion, the furnace power switch was immediately turned off. Subsequently, the column specimens were cooled in the furnace with the door closed. The fire test

Table 5 Fire test results

| Item	Specimen No.			
	A1	A2	B1	B2
Duration of fire test (min)	169	51	112	42
Fire resistance (min)	168	50	111	41
Maximum axial deformation (mm)*	14.8	8.5	7.1	1.6
Time required to reach maximum elongation (min)	19	15	15	11
Average temperature of steel tube upon termination (℃)	-	735.9	809.2	715.0
Maximum temperature of steel tube upon termination (℃)	-	885.3	944.3	842.9
Average temperature of inner concrete upon termination (℃)	-	312.3	-	119.1

* Note: Positive values indicate expansion and negative contraction

results such as fire resistance, maximum axial deformation, average temperature of steel tube upon termination, average temperature of inner concrete upon termination, and maximum temperature of steel tube upon termination are shown in Table 5. As can be seen from Table 5, the CFTC

specimens expanded in the initial stages and then contracted leading to failure. In the initial stages, the effects of load and thermal expansion were significant. While in the later stages, the influence of creep became obvious. This result was similar to those reported by other researchers (Lie and Kodur 1996, Kodur 1999).

As previously stated, the temperature inside the furnace and within the specimens was measured during the fire test. The temperature from the specimen's surface to the inner central core was measured by type K thermocouples located at different depths in four sections of the column (Fig. 2). Throughout the fire test, the temperature of the steel tube and inner concrete rose with the increasing temperature of the furnace. Basically, the rate of temperature rise in steel tube was more rapidly than the concrete core because of its high thermal conductivity and direct exposure to fire. For example, Fig. 8 shows the steel tube temperature versus time curves for the B2 specimen, while Fig. 9 shows the curves of inner concrete temperature versus time for the B2 specimen.

Comparing Fig. 8 with Fig. 9, it can be seen that the temperature rise rate of steel tube was obviously higher than that of the concrete core. Even if the average temperature of the steel tube in the B2 specimen reached 715℃, the average temperature of the inner concrete was only about 119℃ (Table 5). In addition, it can be seen in Table 5 that the measured values of the maximum temperature of the
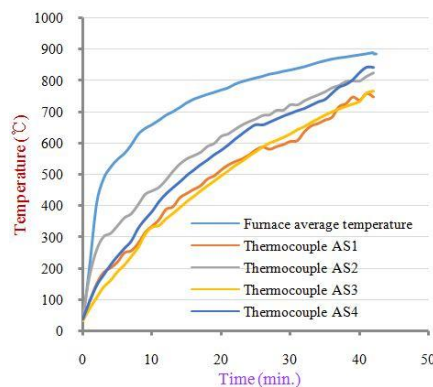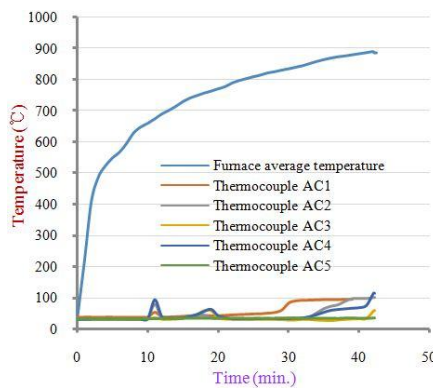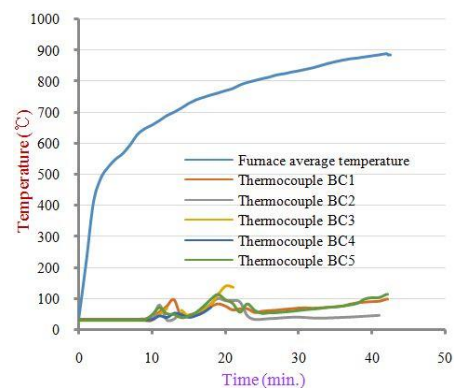

(a) Section A
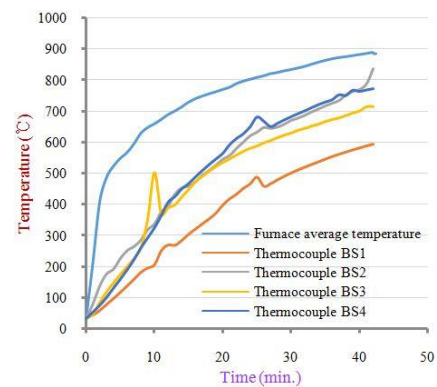
(b) Section B

Fig. 8 Steel tube temperature versus time curves for the B2 specimen

(a) Control group

(b) Experimental group

Fig. 9 Concrete temperature versus time curves for the B2 specimen

steel tube upon shutdown of the furnace were 885.3, 944.3, and 842.9°C for the A2, B1, and B2 specimens, respectively. However, due to the explosive spalling of the inner concrete, the thermometers in the A1 specimen failed after 65 minutes of the fire exposure test, so that the maximum temperature could not be measured correctly.

3.4 Axial deformation

Axial deformations for all the CFTC specimens are shown in Table 6. Positive values indicate an expansion, whereas negative values indicate a contraction. The axial deformation of the columns was measured by LVDTs and displacement meters located outside the furnace. The deformation in these columns was caused by several major factors, such as load, thermal expansion and creep. Overall, with the increase of fire temperature, the axial deformation of the CFTC specimens also increased owing to thermal expansion. When the average temperature of the steel exceeded 500°C, the axial elongation reached its maximum. After that, the axial deformation of the test specimen began to decrease. Afterwards, the specimen contracted until the test was terminated. The contraction in the column length under the applied load resulted from the deterioration of the material properties at elevated temperatures. In other words, the observed axial deformations of the column specimens were the result of a combination of the mechanical and thermal load.

Fig. 10 shows the axial deformation (y-axis) versus time (x-axis) curve recorded during the fire exposure test. It is clear from the figure that due to the thermal expansion behavior of the material, the column underwent an
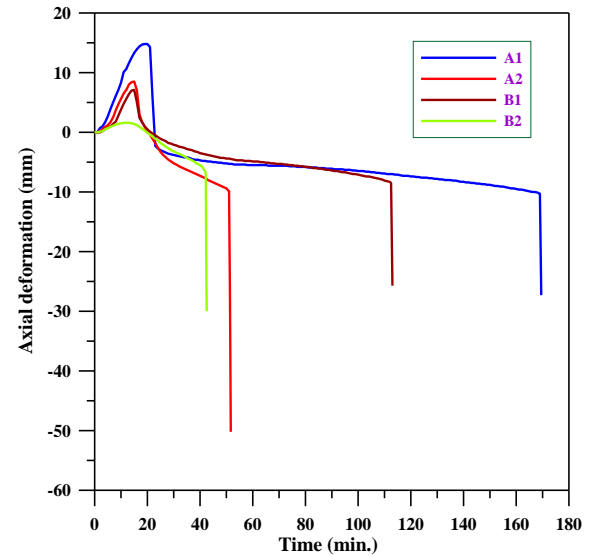

Fig. 10 Axial deformation versus time curves for CFBC specimens

expansion phase before being compressed to failure. Basically, the steel tube heated up faster because of its high thermal conductivity, thus expanding faster than the concrete core (Kodur 2007).

In addition, with the increased fire time, the axial deformation of the CFTC specimens increased up to the maximum elongation. At that point, contraction began immediately, as shown in Fig. 10. Taking the control group as an example, it is shown in Table 6 that during the first 20 minutes in the fire test, the A1 specimen's axial elongation was greater than that of the A2 specimen. The reason is the load level for fire design of the A1 specimen was lower than that of the A2 specimen. As for the experimental group, it can be clearly seen from Table 6 that during the first 15 minutes in the fire test, the B1 specimen's axial elongation was greater than that of the B2 specimen. The reason is the same as above. Under the same load level for fire design, compare the axial deformation of the A2 specimen and the B1 specimen, as shown in Fig. 10. From Fig. 10, it can be seen that the axial deformation of the A2 specimen was larger than that of the B1 specimen. As soon as the test progressed to the compression phase, the contraction of the A2 specimen was also greater than that of the B1 specimen.

Moreover, Fig. 11 shows the axial deformation rate versus time curves for the CFTC specimens. It can be clearly seen in Fig. 11(b) that A2 specimen's axial deformation rate was -16.1 mm/min when the fire duration reached 51 minutes. In other words, the compressive deformation rapidly increased at this moment. In contrast, Fig. 11(a) shows that the A1 specimen was obviously compressed until 169 minutes. Therefore, the A1 specimen had a better fire behavior because the load level for fire design of the A1 specimen was lower than that of the A2 specimen. As for the experimental group, it can be clearly seen from Fig. 11(c) that the B1 specimen was obviously compressed until 112 minutes. Compared with the B1 specimen, the B2 specimen's axial deformation rate was -14.1 mm/min when the fire duration reached 42 minutes. In other words, the B1 specimen had a better fire behavior

Table 6 Axial deformation for CFTC specimens

Fire duration (min.)	Axial deformation (mm)			
	A1 specimen	A2 specimen	B1 specimen	B2 specimen
5	2.7	1.2	0.8	0.9
10	8.3	5.6	3.8	1.6
15	13.3	8.5	7.1	1.2
20	14.8	0.2	0.5	-0.4
25	-3.0	-3.3	-1.1	-2.1
30	-3.8	-5.2	-2.1	-3.4
35	-4.2	-6.3	-2.8	-4.5
40	-4.7	-7.3	-3.5	-5.9
45	-5.0	-8.4	-4.0	-
50	-5.2	-9.4	-4.4	-
60	-5.5	-	-4.9	-
70	-5.6	-	-5.3	-
80	-5.8	-	-5.8	-
90	-6.1	-	-6.4	-
100	-6.5	-	-7.1	-
110	-6.9	-	-8.1	-
160	-9.5	-	-	-

* Note: Positive values indicate expansion and negative contraction

(a) A1 specimen

(b) A2 specimen
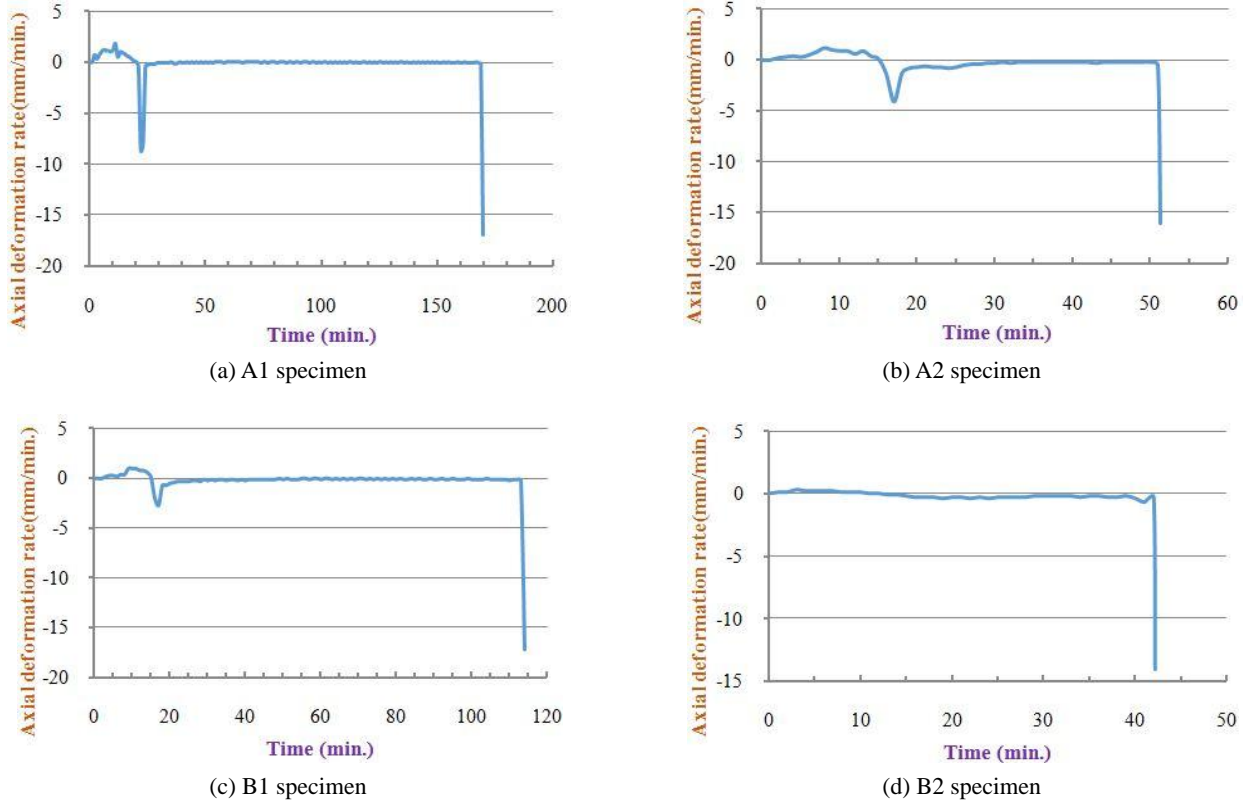

(c) B1 specimen

(d) B2 specimen

Fig. 11 Axial deformation rate versus time curves for the CFTC specimens
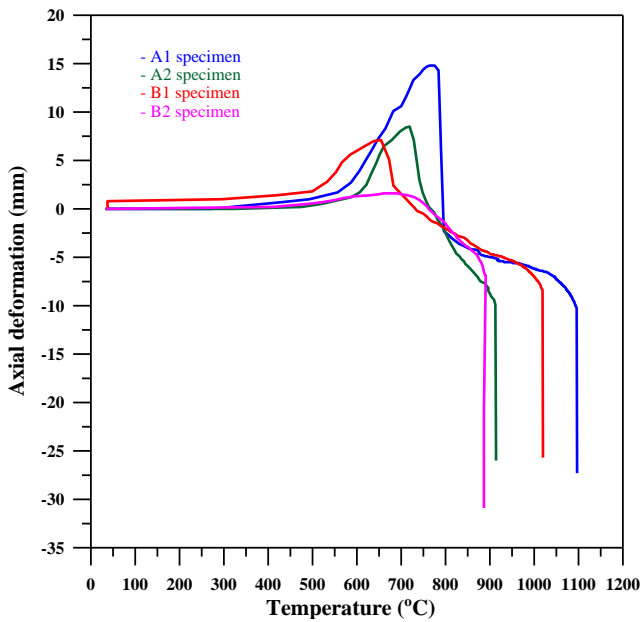

Fig. 12 Axial deformation versus temperature curves for CFTC specimens

because the load level for fire design of the B1 specimen was lower than that of the B2 specimen.

On the other hand, Fig. 12 shows the axial deformation versus temperature for all the CFTC specimens. Because of the different load levels for fire design of the specimens, the relationship between the axial deformation and the average temperature inside the furnace was also different. As can be seen in Fig. 12, the specimens began to elongate when the average furnace temperature reached about 300℃; the axial elongation of the specimens increased rapidly when the average furnace temperature was between 600-790℃; the axial compressive deformation sharply increased in a very short time when the average furnace temperature was between 880-1090℃. Taking the A1 specimen as an example, when the average furnace temperature was about 300℃, the specimen began to elongate. Before the average furnace temperature reached 500℃, the axial deformation of the specimen A1 was less than 1 mm. When the average furnace temperature was between 500 and 680℃, the axial deformation of the test specimen gradually increased, but its value was less than 10 mm. When the average furnace temperature was between 680 and 765℃, the axial elongation of the test specimen increased rapidly. When the average furnace temperature was about 765℃, the axial deformation of the specimen reached a maximum value (14.8 mm). When the average furnace temperature was between 765 and 790℃, the test specimen stopped its elongation and began to rapidly contract. When the average furnace temperature was about 790℃, the test specimen axial deformation was zero. When the average furnace temperature was between 790 and 1000℃, the axial compressive deformation of the test specimen gradually increased. When the average furnace temperature was between 1000 and 1090℃, the axial compressive deformation of the test specimen increased sharply. The average furnace temperature was about 1096℃, the specimen axial compression deformation had reached 27 mm.
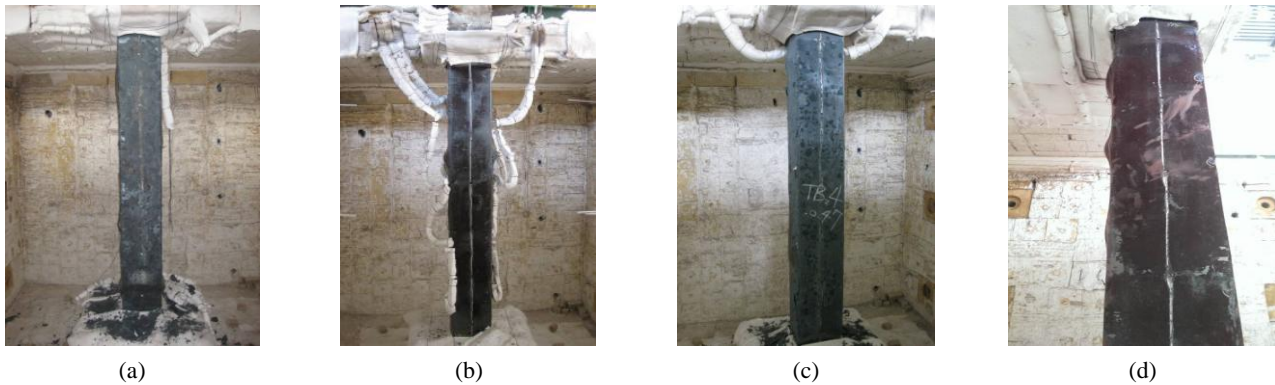
Fig. 13 A general view of specimens after fire test: (a) A1, (b) A2, (c) B1, and (d) B2 specimens

3.5 Fire resistance

Taking the control group as an example, it can be seen from Table 5 that the fire resistance of the A1 specimen was obviously better than that of the A2 specimen. The main reason is that the load level for fire design of the A1 specimen was lower than that of the A2 specimen. As for the experimental group, it can be clearly seen from Table 5 that the fire resistance of the B1 specimen was also significantly better than that of the B2 specimen. The reason is as described above. Under the same load level for fire design, compare the fire resistance of the A2 specimen and the B1 specimen, as shown Table 5. From Table 5, it can be seen that the fire resistance of the B1 specimen was 111 minutes, as compared with 50 minutes for the A2 specimen. In other words, the fire resistance of the B1 specimen was obviously better than that of the A2 specimen. The main difference was that the experimental group was equipped with longitudinal reinforcement and transverse stirrups. Therefore, it can be concluded that the presence of rebars not only decreased the spread of cracks and the sudden loss of strength, but also contributed to the load-carrying capacity of the concrete core. This result shows that the configuration of longitudinal reinforcements and transverse stirrups can significantly improve the fire resistance of CFTCs.

The tabular data design method described in EN 1994-1-2: 2005 – chapter 4.2 for the case of centrally loaded concrete filled steel tubular hollow sections was reviewed. In this study, the design and test parameters of the CFTC specimens complying with the load bearing criterion for different minutes in standard fire exposure are shown in Table 2, and the test results are shown in Table 5. A comparison of Tables 1 and 5 shows that the fire resistance of the CFTC specimens was consistent with or above the recommended values of Eurocode 4's tabulated data. In other words, Eurocode 4's tabular data is fairly credible, but conservative. Taking the B1 specimen as an example, it's fire resistance was 111 minutes. According to Eurocode 4's tabulated data, it's fire rating was R90.

On the other hand, from the beginning to the end of the fire test, except for the B2 specimen, the other specimens emitted several clear bursts of sound. Taking the A1 specimen as an example, when the fire exposure test progressed to the 21st minute (the average furnace

temperature was about 780℃), the cracking sound came from the specimen inside the furnace; it continued to burst even when it was heated to the 108th minute. After the heating process, the CFTC specimens were allowed to cool slowly to room temperature in the furnace. Then, their failure modes were further observed. Overall, the failure was either by local buckling or general instability. Fig. 13 shows the appearance of the A1, A2, B1, and B2 specimens after the fire test. It can be clearly seen that the final failure mode was the local bulge of the steel tubes. As demonstrated in Fig. 13, the local bulge of the steel tubes occurred at several locations were observed. Taking the A2 specimen as an example, it can be seen from Fig. 13(b) that a prominent bulge was observed in the web near the intermediate height of the column.

4. Conclusions

Results from fire resistance experiments on four CFTC specimens are presented in this paper. The B2 specimen did not burst because of its higher load level for fire design. However, when the average temperature inside the furnace was about 780℃, the remaining specimens started to burst immediately. Overall, CFTCs have excellent structural behavior. The filling of concrete or reinforced concrete can increase the rigidity of the steel tube. In addition, it provides a practical solution for hollow structural steel columns without the need for external fire protection. On the basis of the above experimental results and discussion, the following conclusions were drawn:

- The CFTC specimens began to elongate when the average furnace temperature reached about 300℃; the axial elongation of the specimens increased rapidly when the average furnace temperature was between 600-790℃; the axial compressive deformation sharply increased in a very short time when the average furnace temperature the was between 880-1090℃.
- The fire resistance of the A1 specimen was 168 minutes, as compared with 50 minutes for the A2 specimen. In addition, the fire resistance of the B1 specimen was 111 minutes, as compared with 41 minutes for the B2 specimen. These results indicate

that the load level for fire design is an important factor affecting the fire resistance of CFTCs. In other words, the higher the load level for fire design, the worse the fire resistance.

- Under the same load level for fire design, the fire resistance of the B1 specimen was 111 minutes, as compared with 50 minutes for the A2 specimen. Therefore, it can be concluded that the configuration of longitudinal reinforcements and transverse stirrups can significantly improve the fire resistance of CFTCs.
- The fire resistance of the CFTC specimens was consistent with or above the recommended values of Eurocode 4's tabulated data. In other words, Eurocode 4's tabular data is fairly credible, but conservative.

References

ACI 363R-92 (1992), State-of-the-Art Report on High-Strength Concrete, ACI Committee 363 Report, American Concrete Institute, Detroit, MI, USA.

ACI-318 (2014), Building code requirements for reinforced concrete and commentary, American Concrete Institute, Farmington Hills, MI, USA.

Aslani, F., Uy, B., Tao, Z. and Mashiri, F. (2015), "Predicting the axial load capacity of high-strength concrete filled steel tubular columns", *Steel Compos. Struct., Int. J.*, **19**(4), 967-993.

ASTM C192/C192M-16a (2016), Standard Practice for Making and Curing Concrete Test Specimens in the Laboratory; ASTM International, West Conshohocken, PA, USA.
URL: www.astm.org

ASTM E119 (2008), Standard Test Methods for Fire Tests of Building Construction and Materials, American Society for Testing and Materials, Philadelphia, CA, USA.

Castillo, C. and Durrani, A.J. (1990), "Effect of transient high temperature on high-strength concrete", *ACI Mater. J.*, **87**(1), 47-53.

Chen, H.J., Yang, Y.C., Tang, C.W. and Peng, C.F. (2017), "Residual-Load-Bearing Capacity of High-Performance Concrete-Filled Box Columns after Fire", *Sens. Mater.*, **29**(4), 523-532.

Ding, J. and Wang, Y.C. (2008), "Realistic modelling of thermal and structural behaviour of unprotected concrete filled tubular columns in fire", *J. Constr. Steel Res.*, **64**, 1086-1102.

Ekmekyapar, T. (2016), "Experimental performance of concrete filled welded steel tube columns", *J. Constr. Steel Res.*, **117**, 175-184.

EN 1992-1-2 (2004), Eurocode 2: Design of concrete structures. Part 1-2: general rules—structural fire design, European Committee for Standardization, Brussels, Belgium.

EN 1994-1-2 (2005), Eurocode 4: Design of composite steel and concrete structures–Part 1-2: General–Structural fire design.

Espinos, A., Hospitaler, A. and Romero, M.L. (2009), "Fire resistance of axially loaded slender concrete filled steel tubular columns", *Acta Polytechnica*, **49**(1), 39-43.

Han, L.H., Yao, G.H. and Zhao, X.L. (2005), "Tests and calculations for hollow structural steel (HSS) stub columns filled with self-consolidating concrete (SCC)", *J. Constr. Steel Res.*, 61, 1241-1269.

Hertz, K.D. (2003), "Limits of spalling of fire-exposed concrete", *Fire Safety J.*, **38**(2), 103-116.

Hong, S. and Varma, A.H. (2009), "Analytical modeling of the standard fire behavior of loaded CFT columns", *J. Constr. Steel Res.*, **65**(1), 54-69.

Jagannath, L., Harish Kumar, N.R., Nagaraja, K.P. and Prabhakara, R. (2016), "Behaviour of normal strength concrete and high strength concrete subjected to in-plane shear", *Int. J. Innov. Res. Sci. Eng. Technol.*, **5**(7), 12242-12251.

Khan, Q.S., Sheikh, M.N. and Hadi, M.N.S. (2016), "Axial compressive behaviour of circular CFFT: Experimental database and design-oriented model", *Steel Compos. Struct., Int. J.*, **21**(4), 921-947.

Kim, D.K., Choi, S.M., Kim, J.H., Chung, K.S. and Park, S.H. (2005), "Experimental study on fire resistance of concrete-filled steel tube column under constant axial loads", *Steel Struct.*, **5**(4), 305-313.

Kodur, V.K.R. (1999), "Performance-based fire resistance design of concrete-filled steel columns", *J. Constr. Steel Res.*, **51**(1), 21-36.

Kodur, V.K.R. (2007), "Guidelines for fire resistant design of concrete-filled steel HSS columns-state-of-the-art and research needs", *Steel Struct.*, **7**, 173-182.

Kodur, V. (2014), "Properties of concrete at elevated temperatures", *ISRN Civil Engineering Volume*, Article ID 468510.

Kodur, V.K.R. and Sultan, M.A. (2003), "Effect of temperature on thermal properties of high-strength concrete", *J. Mater. Civil Eng.*, **5**(2), 101-107.

Kodur, V.K.R., Wang, T.C. and Cheng, F.P. (2004), "Predicting the fire resistance behavior of high strength concrete columns", *Cement Concrete Compos.*, **26**(2), 141-153.

Krzemień, K. and Hagera, I. (2009), "Assessment of concrete susceptibility to fire spalling: A report on the state-of-the-art in testing procedures", *Procedia Eng.*, **108**, 285-292.

Lavanya, J. and Elangovan, R. (2017), "The structural behaviour of concrete filled steel tubular columns", *Int. Res. J. Eng. Technol.*, **4**(6), 209-215.

Lie, T.T. and Kodur, V.K.R. (1996), "Fire resistance of steel columns filled with bar-reinforced concrete", *ASCE J. Struct. Eng.*, **122**(1), 30-36.

Liew, J.Y.R. and Xiong, M. (2015), *Design Guide for Concrete Filled Tubular Members with High Strength Materials to Eurocode 4*, Research Publishing, Blk 12 Lorong Bakar Batu, #2-11, 349568, Singapore.

Liu, Y.X., Tong, G.S. and Zhang, L. (2015), "Fire resistance and load-bearing capacity of concrete filled fire-resistant steel tubular columns with circular cross-section", *J. Zhejiang Univ. (Eng. Sci.)*, **49**(2), 208-217.

Mago, N. and Hicks, S.J. (2016), "Fire behaviour of slender, highly utilized, eccentrically loaded concrete filled tubular columns", *J. Constr. Steel Res.*, **119**, 123-132.

Mundhada, A.R. and Pofale, A.D. (2015), "Effect of high temperature on compressive strength of concrete", *IOSR J. Mech. Civil Eng.*, **12**(1), 66-70.

Phan, L.T. and Carino, N.J. (1998), "Review of mechanical properties of HSC at elevated temperature", *J. Mater. Civil Eng.*, **10**(1), 58-64.

Phan, L.T. and Carino, N.J. (2002), "Effects of test conditions and mixture proportions on behavior of high-strength concrete exposed to high temperatures", *ACI Mater. J.*, **99**(1), 54-66.

Purkiss, J.A. (2007), *Fire Safety Engineering Design of Structures*, Butterworth-Heinemann, Elsevier, Oxoford, UK.

Qu, X., Chen, Z., Nethercot, D.A., Gardner, L. and Theofanous, M. (2015), "Push-out tests and bond strength of rectangular CFST columns", *Steel Compos. Struct., Int. J.*, **19**(1), 21-41.

Sanjayan, G. and Stocks, L.J. (1993), "Spalling of high-strength silica fume concrete in fire", *ACI Mater. J.*, **90**(2), 170-173.

Schaumann, P. and Kleibömer, I. (2017), "Experimental and numerical investigations of the composite behaviour in concrete-filled tubular columns with massive steel core at high temperatures", *J. Struct. Fire Eng*.
DOI: https://doi.org/10.1108/JSFE-01-2017-0010

Siddique, R. and Kaur, D. (2012), "Properties of concrete containing ground granulated blast furnace slag (GGBFS) at elevated temperatures", *J. Adv. Res.arch*, **3**(1), 45-51.

Song, T.Y., Han, L.H. and Yu, H.X. (2010), "Concrete filled steel tube stub columns under combined temperature and loading", *J. Constr. Steel Res.*, **66**(3), 369-384.

Tan, K. and Nichols, J.M. (2017), "Properties of high-strength concrete filled steel tube columns", *Modern Civil Struct. Eng.*, **1**(1), 58-77. DOI: 10.22606/mcse.2017.11005

Tang, C.W. (2017), "Fire resistance of high strength fiber reinforced concrete filled box columns", *Steel Compos. Struct., Int. J.*, **23**(5), 611-621.

Tang, C.W. and Chen, C.Y. (2017), "Fire Resistance of Concrete-Filled Box Columns Fabricated with Different Welding Methods", *Sens. Mater.*, **29**(4), 371-377.

Taiwan Construction and Planning Agency (2004), Design Code and Commentary for Steel Reinforced Concrete Structures, Taipei. [In Chinese]

Tao, Z., Ghannama, M., Song, T.Y. and Han, L.H. (2016), "Experimental and numerical investigation of concrete-filled stainless steel columns exposed to fire", *J. Constr. Steel Res.*, **118**, 120-134.

Uy, B. (2001), "Strength of short concrete filled high strength steel box columns", *J. Constr. Steel Res.*, **57**(1), 113-134.

Wan, C.Y. and Zha, X.X. (2016), "Nonlinear analysis and design of concrete-filled dual steel tubular columns under axial loading", *Steel Compos. Struct., Int. J.*, **20**(3), 571-597.

Xiong, M.X. and Liew, J.Y.R. (2016), "Mechanical behaviour of ultra-high strength concrete at elevated temperatures and fire resistance of ultra-high strength concrete filled steel tubes", *Mater. Des.*, **104**, 414-427.

Zhou, X., Mou, T., Tang, H. and Fan, B. (2017), "Experimental study on ultrahigh strength concrete filled steel tube short columns under axial load", *Adv. Mater. Sci. Eng.* Article ID 8410895, 9 p. DOI: https://doi.org/10.1155/2017/841089

CC